

# Parallel Invaded Cluster Algorithm for the Ising Model

Y. S. Choi and J. Machta

*Department of Physics and Astronomy, University of Massachusetts, Amherst, MA 01003-3720*

P. Tamayo

*Thinking Machines Corp., Bedford, MA 01730*

L. X. Chayes

*Department of Mathematics, University of California, Los Angeles, CA 90095-1555*

(November 15, 2018)

## Abstract

A parallel version of the invaded cluster algorithm is described. Results from large scale (up to  $4096^2$  and  $512^3$ ) simulations of the Ising model are reported. No evidence of critical slowing down is found for the three-dimensional Ising model. The magnetic exponent is estimated to be  $2.482 \pm .001$  ( $\beta/\nu = 0.518 \pm .001$ ) for the three-dimensional Ising model.

## I. INTRODUCTION

Advances in algorithms and hardware have greatly increased the power and scope of Monte Carlo studies of critical phenomena. Cluster algorithms, first introduced by Swendsen and Wang [1], largely overcome the problems of critical slowing and thereby permit the study of very large systems using a reasonable number of Monte Carlo steps. Parallel machines provide platforms on which very large systems may be efficiently studied. Several groups [2–4] have implemented cluster algorithms on parallel machines to obtain high precision results for the three-dimensional Ising model.

The invaded cluster (IC) algorithm [5,6] is a new type of cluster algorithm with features that make it very attractive for high precision studies of critical phenomena. First, it has less critical slowing than other cluster algorithms. Indeed, here we provide strong evidence that for the three-dimensional Ising model there is no critical slowing down. Second, the IC algorithm does not use an estimate of the critical temperature as an input; instead, the critical point is sampled without any fine-tuning of parameters and an estimate of the critical temperature is obtained as an *output* of the simulation. On the other hand, the IC algorithm samples the IC ensemble rather than the canonical ensemble. Although the two ensembles are believed to be equivalent in the infinite volume limit, the finite-size scaling properties of the IC ensemble are not yet well-understood. Here we present results that test a simple finite-size scaling hypothesis and determine the associated finite-size scaling exponent.

In this paper we describe an implementation of the invaded cluster algorithm for distributed memory SPMD (single program multiple data) parallel machines. Using this algorithm we studied two- and three-dimensional Ising systems up to size  $4096^2$  and  $512^3$ , respectively. There are several motivations for this project. The first is to develop an efficient implementation of the IC method for parallel computation. This is a non-trivial problem because the IC method appears to be quite sequential. The second objective is to better understand the dynamics of the IC algorithm and the finite-size scaling properties of the IC ensemble. These properties are interesting in their own right and they must be understood before the algorithm can be used for high-precision studies. Finally, we wish to obtain accurate results for the critical temperature and exponents for the three-dimensional Ising model. With relatively modest effort we have been able to obtain accuracy comparable to recent studies in the measurement of  $\beta/\nu$  and somewhat less accuracy for the critical temperature. We argue that the IC method is likely to be the most efficient method for obtaining very high precision estimates for the critical temperature and the magnetic exponent for the Ising model and related spin systems.

In Sec. II we describe the invaded cluster method and discuss our parallel implementation. In Sec. III we discuss the performance of the parallel IC algorithm running on CM-5 machines. In Sec. IV we present some high-precision numerical results for the three-dimensional Ising model using the parallel IC algorithm. Conclusions are presented in Sec. V.

## II. INVADDED CLUSTER ALGORITHM

### A. Cluster Methods

In cluster Monte Carlo methods a spin system is sampled in both its spin representation and in an associated *graphical representation*. The graphical representation is an interacting percolation model that is usually defined on the bonds of the lattice. The graphical representation by itself contains all of the information relevant for the study of the spin system. A single Monte Carlo (MC) step consists of two parts, a ‘bond move’ and a ‘spin move.’ During the bond move, the spins are frozen and the graphical configuration (bond configuration) is updated in accord with the current spin configuration. During the spin move, it is the opposite: the bonds are frozen and the spin configuration is updated. In a critical region, tremendous improvements in the efficiency of cluster methods over traditional local dynamics can arise if the graphical representation has a coinciding percolation threshold. In this case, clusters of spins on all scales are coherently updated.

Since the IC and Swendsen-Wang (SW) algorithms are very similar let us begin with a brief description of the SW algorithm. Consider the nearest neighbor Ising magnet on the square or cubic lattice defined by the Hamiltonian

$$\beta H = -K \sum_{\langle i,j \rangle} \sigma_i \sigma_j \quad (1)$$

where  $\sigma_i = \pm 1$ ,  $K$  is the dimensionless coupling, and the sum is over all the bonds of the lattice. During the bond move, each ‘satisfied’ bond ( $\langle i,j \rangle$  is satisfied if  $\sigma_i = \sigma_j$ ) is independently occupied with probability  $p$  or left vacant with probability  $(1-p)$ . Unsatisfied

bonds are never occupied. After a bond configuration has been created in this fashion, *clusters* are identified: A cluster is a set of (like) spins connected by occupied bonds; an isolated spin is also counted as clusters. Next, the spin configuration is erased and the bond move is completed. The spin move for the SW algorithm consists of assigning either spin-up or spin-down with probability 1/2 independently to every cluster. Each spin in the cluster takes the spin value assigned to the cluster and then the bond configuration is erased and the spin move is completed. The SW algorithm samples the canonical ensemble at coupling  $K$  where  $K$  is related to  $p$  via

$$p = p(K) \equiv 1 - e^{-2K}. \quad (2)$$

The spin move for the IC algorithm is the same as for the SW algorithm: each cluster is assigned either spin-up or spin-down with probability 1/2. The IC bond move consists of occupying the satisfied bonds in random order until the cluster configuration first fulfills a stopping rule. During the bond move, bonds are occupied one at a time and after each bond is added, the cluster structure is checked to see if the stopping rule is satisfied. There are a number of useful stopping rules, some of which, evidently, cause the algorithm to sample the Ising critical point. In this study, we will use ‘topological’ rules which are appropriate for systems with periodic boundary conditions. There are several versions: The ‘1-span’ topological rule demands that some cluster is connected around the system in at least one of the periodic directions – as soon as this condition is fulfilled, the bond move is complete and no more bonds are added to the configuration. In general, the  $k$ -span rule ( $k \leq d$ ) requires that there is connectivity around the system in at least  $k$  directions. Although all of the  $k$ -span rules sample the Ising critical point, the different rules have different finite-size scaling behavior.

The critical coupling and the magnetic exponent may be obtained in the IC approach. We begin with  $K_c$ . Let  $f$  be the ratio of the number bonds occupied during the bond move to the number of satisfied bonds for a single Monte Carlo (MC) step. The average value of  $f$  is an estimator of the critical temperature according to the relation

$$\lim_{L \rightarrow \infty} \langle f \rangle = 1 - e^{-2K_c} \quad (3)$$

where  $K_c$  is the critical coupling and  $L$  is the system size. To understand this relation, note that the only difference between the SW and IC algorithms is the way in which  $f$  is determined in a bond move. For the SW algorithm, each satisfied bond is independently occupied with probability  $p$  so that the ratio of occupied to satisfied bonds is a binomial random variable. For the IC algorithm, the stopping rule determines the number of occupied bonds. However, for large systems, one can presume that the fluctuations in  $f$  become small for both algorithms. As a consequence, the IC algorithm that outputs  $\langle f \rangle$  yields the same value for all local observables as the SW algorithm with  $p(K) = \langle f \rangle$  so that the relation  $\langle f \rangle \simeq 1 - e^{-2K}$  yields an estimate of the temperature of the IC ensemble. The bond percolation threshold on the set of satisfied bonds at the Ising critical point is known to be  $p(K_c)$ . Since the  $k$ -span rules forces the cluster configuration to the percolation threshold, we see that Eq. (3) holds. This argument (which still lacks a rigorous proof) is discussed in more detail in Ref. [6]

Let us now turn to a discussion of the magnetic exponent. For a critical stopping rule, such as a topological rule, the cluster that fulfills the stopping condition is called the *spanning*

*cluster*. This spanning cluster can be thought of as a typical example of a large-scale cluster at criticality and thus its fractal dimension yields the magnetic exponent for the system. In particular, if  $M$  is the number of sites in the spanning cluster, we determine the fractal dimension  $D$  via

$$M \sim L^D \quad (4)$$

The fractal dimension is related to other critical exponents via  $D = y_h = d - \beta/\nu$  where  $y_h$  is the magnetic exponent,  $\beta$  the magnetization exponent,  $\nu$  the correlation length exponent and  $d$  the spatial dimension. At the present time we do not know how to extract the thermal exponent from the IC algorithm.

The finite-size scaling properties of the IC ensemble are currently under investigation. Here we state the fundamental assumption that will be used later in the analysis of the data. Let  $\mathcal{F}(f, L)$  be the (cumulative) distribution function for  $f$  measured in a system of size  $L$ . We suppose that there is an exponent,  $u$  and function  $\mathcal{G}$  such that

$$\mathcal{F}(f, L) \sim \mathcal{G}[(f - p(K_c))L^u] \quad (5)$$

Naive finite-size scaling arguments suggest that  $u = 1/\nu$  with  $\nu$  the Ising correlation length exponent, however it is quite apparent that this is not the case. Measurements of  $u$  reported in Ref. [6] and below in Sec. IV yield a value  $u \approx 0.69$  in  $d = 3$ . Presumably this  $u$  is the inverse of the correlation length exponent for a related percolation-Ising hybrid model but at present, no definitive conclusions have been obtained.

## B. Parallelizing the Invaded Cluster Algorithm

The approach taken here to parallelize the IC algorithm is based upon the parallel SW algorithm described in Ref. [3]. The basic idea for both algorithms is to divide the lattice into cells each of which is handled by a single processor. During the bond move the cluster configuration must be determined. Every site of the lattice has an integer label that identifies its cluster membership. Two sites are in the same cluster if they have the same label. At the beginning of the bond move, every site has a unique local label. The SW bond move proceeds in two stages. In the *local* stage, each processor in parallel occupies a fraction  $p$  of the satisfied bonds in its cell and identifies the local cluster structure using a conventional sequential method. The local clusters are the clusters that would exist if no bonds on the boundaries of the cell were occupied. During the *relaxation* stage, global labels are created and global clusters are identified. Global clusters which are formed out of local clusters by boundary connections between cells are assigned the lowest valued label from the the labels of the connected local clusters. This is accomplished iteratively by the exchange of labels between neighboring cells. A very similar relaxation stage is used for the IC algorithm except that more information must be exchanged between nodes to allow for checking the stopping condition.

Since communication between processing nodes is much slower than processes handled by a single node it is desirable that individual nodes do as much work as possible between communication steps. On the other hand, the sequential IC algorithm checks for spanning after each new bond is occupied. Clearly this would not be a good approach to directly

parallelize. Instead, the algorithm converges to the value of  $f$  by a sequence of choices of  $p$ . Imagine that an independent uniform random number between 0 and 1 is assigned to each bond of the lattice. (In fact, this is not quite the approach that is actually used but, for purposes of explanation, suppose that this is the case.) On the first step each processor provisionally occupies all satisfied bonds with random numbers less than  $p_1$ . The resulting cluster configuration is identified and the stopping rule is checked. For the sake of argument, suppose that spanning is not detected. In this case, the provisionally occupied bonds are permanently occupied and a new value  $p_2 > p_1$  is chosen. The current cluster configuration is stored and additional bonds are provisionally occupied with random numbers from  $p_1$  to  $p_2$ . The cluster configuration is modified accordingly and the stopping condition is checked. If spanning is not detected, the new cluster configuration is stored and the provisionally occupied bonds given tenure. The value of  $p$  is incremented in this way until on the  $s$ th step the stopping condition is fulfilled. At this point we know that spanning occurs between  $p_{s-1}$  and  $p_s$ . We backtrack to the cluster configuration (saved in memory) associated with  $p_{s-1}$  and try again, this time choosing  $p = (p_{s-1} + p_s)/2$ . Henceforth, the algorithm carries out a binary search, each time reducing the range of  $p$  by half until the stopping condition is just fulfilled and  $f$  is determined.

In the above discussion we supposed that random numbers are assigned to each bond and that on each step all satisfied bonds with random numbers less than  $p$  are occupied. This is not an efficient procedure because it requires examining every bond each time  $p$  is changed. Instead we do the following. Each processor creates a random permutation of the  $n$  bonds in its cell. This permutation determines the order in which bonds will be tested by the processor. On the first step, processor  $i$  tests its first  $h_i^{(1)}$  bonds where  $h_i^{(1)}$  is chosen from the binomial distribution,  $\mathcal{B}[n, p_1]$  for  $n$  trials with success probability  $p_1$ . This is statistically equivalent to testing all bonds with random numbers less than  $p_1$  as described in the previous paragraph. Suppose that spanning is not found, then  $p_1$  is incremented to  $p_2$ . At this point processor  $i$  has permanently occupied  $a_i^{(1)} \leftarrow h_i^{(1)}$  bonds. Processor  $i$  now tests the next  $h_i^{(2)}$  bonds where now  $h_i^{(2)}$  is chosen from  $\mathcal{B}[n - a_i^{(1)}, (p_2 - p_1)/(1 - p_1)]$ . This process of occupying bonds continues as long as the stopping condition is not fulfilled and on the  $m$ th such step the number of occupied bonds is incremented according to  $a_i^{(m)} \leftarrow a_i^{(m-1)} + h_i^{(m)}$ . Suppose that spanning is first detected on step  $s$  and that  $h_i^{(s)}$  bonds have been provisionally occupied by processor  $i$  during this step. On the next step each processor tries to occupy a smaller number of bonds corresponding to splitting the difference between  $p_{s-1}$  and  $p_s$ . To do this, processor  $i$  tests the next  $h_i^{(s+1)}$  bonds starting with the  $(a_i^{(s-1)} + 1)$ th bond where  $h_i^{(s+1)}$  is chosen from  $\mathcal{B}[h_i^{(s)}, 1/2]$ . A little reflection shows that this procedure is statistically equivalent to the one described above for carrying out the binary search. The advantage of this approach is that on successive steps it is not necessary to check every bond in the cell. Note that the local ordering of bonds is fully specified at the outset of the bond move but that the global ordering of the bonds is generated as needed and never fully specified.

### III. PERFORMANCE

We tested the parallel IC algorithm for the two-dimensional Ising model on a 32-node CM-5 machine. Fig. 1 shows that the number of relaxation cycles  $n_{\text{relax}}$  per MC step as a

function of system size  $L$ . The roughly logarithmic increase in  $n_{\text{relax}}$  results from the binary search method used to find  $f$ . We separately measured the time spent in local cluster growth  $t_{\text{local}}$  and relaxation  $t_{\text{relax}}$ . The local time increases as the number of spins per node, thus, for a fixed number of processors,  $t_{\text{local}} \sim L^d$ . The relaxation time is dominated by communication between nodes so  $t_{\text{relax}}$  is proportional to the boundary area of the local lattice and the number of relaxation cycles,  $t_{\text{relax}} \sim L^{d-1} \log L$ . Fig. 2 shows local and relaxation times as a function of system size. The relaxation time is greater for small systems but, when the number of spins per node exceeds several hundred thousand the local time dominates.

In Fig. 3 we compare the performance of the parallel IC algorithm with that of the parallel SW algorithm for the two-dimensional Ising model. The total time per spin per MC step for both algorithms decreases as the system size increases and saturates for large systems. For large systems in both two and three dimensions, the time for one MC step for the parallel IC algorithm is about a factor of 7 larger than for the parallel SW algorithm.

We obtained 1.1  $\mu$  s per spin per MC step for the parallel IC algorithm for the two-dimensional Ising models with system size  $4096^2$  on the 32-node CM-5 machine and 3.4  $\mu$  s per spin per MC step for the three-dimensional Ising model on the same machine and with the same number of spins ( $256^3$ ). The slower speed for three-dimensions results from the need for more communications between nodes since each node has six neighbors rather than four. For both two and three dimensions the time per spin per MC step decreases as the system size increases. The relaxation time is, however, still comparable to the local time for  $256^3$ , so the parallel IC algorithm for the three-dimensional Ising model can be expected to become more efficient as the system size increases holding the number of processors fixed.

To test the sensitivity of the algorithm to the random number generator, we performed simulations using two different random number generators. Most of the data is collected using the 250-shift generator in which new random numbers are produced by  $X_i = X_{i-103} \oplus X_{i-250}$ , where  $X_i$  are 32-bit integers and  $\oplus$  represents the bitwise exclusive OR operation. We also tested a combined shift register generator, introduced in Ref. [8]. The combined generator consists of two shift registers  $a_i = a_{i-9218} \oplus a_{i-9689}$  and  $b_i = b_{i-97} \oplus b_{i-127}$  with 32-bit integers  $a_i, b_i$ . New random numbers of the generator are combined by  $X_i = a_i \oplus b_i$ . We observed no difference between results from the two generators. For example, the mean value of  $f$  for system size  $80^3$  was measured as  $.358\ 144 \pm .000\ 006$  for the first generator and  $.358\ 143 \pm .000\ 003$  for the second.

#### IV. NUMERICAL RESULTS

We studied the three-dimensional Ising model using the parallel IC algorithm for system sizes  $16^3$  to  $512^3$ . Unless otherwise stated we used the 1-span rule. For each run we allowed 200 MC steps for equilibration before collecting data. Independent runs consisted of 10 000 MC steps for the smallest systems (up to  $96^3$ ) to 500 MC steps for the largest system ( $512^3$ ). For each size, a number of independent runs were made. We obtained statistics for  $f$  and the size of the spanning cluster. Error bars represent the standard error (one standard deviation) associated with these independent runs. The data for the 1-span rule is given in Table I.

Figure 4 is a double logarithmic plot of  $\sigma_f = (\langle f^2 \rangle - \langle f \rangle^2)^{1/2}$  vs. system size. A fit of the form  $\sigma_f = a + bL^{-u}$ , yields  $a = 0.0003 \pm .0002$  and  $u = 0.69 \pm .01$ . This result

strongly supports the hypothesis that  $\sigma_f$  approaches zero as a power law.

The finite-size scaling hypothesis, Eq. (5) implies an asymptotically linear relation between  $\langle f \rangle$  and  $\sigma_f$ . Figure 5 shows plots of  $\langle f \rangle$  against  $\sigma_f$  for the three  $k$ -span rules. Although these plots are consistent with asymptotic linear behavior, it is clear that there are large subleading corrections to scaling. For the 1-span rule these corrections are negative and for the 3-span rule they are positive.

Figure 6 shows more detail for the 1-span rule where, over the range of system sizes studied,  $\langle f \rangle$  varies only in the fifth significant digit. However, to obtain yet higher accuracy than  $p(K_c) = .3581$  requires either larger system sizes or a good fit to the subleading terms. Fitting to the form  $\langle f \rangle = p(K_c) + a\sigma_f + b\sigma_f^2$  we obtain  $p(K_c) = 0.358\,068 \pm .000\,009$  with  $a = .021$  and  $b = -1.47$ . The corresponding critical coupling, quoted with two standard deviation errors, is  $K_c = 0.221\,637 \pm .000016$ . The fit is shown as a dotted line in the figure. The primary difficulty in obtaining a high precision value of the critical coupling is the relatively large corrections to scaling, represented by the fact that the fitting parameter  $b$  is a good deal larger than  $a$ . Our estimate of the critical coupling is consistent with recent values [4,7,8] (e.g.  $K_c = 0.221\,654\,6 \pm .000\,001$  [8]) but the error is much larger.

Figure 7 shows the median value of  $f$  for the 1-span rule versus  $\sigma_f$ . According to the finite-size scaling hypothesis this plot should also be linear and, indeed, approximately linear behavior is evidenced over the whole range of system sizes however it should be noted that the variation in the median is much larger than for the mean. Furthermore, errors in the mean are less. Thus appears that the mean is a better estimator of the critical coupling.

We measured the mass (the number of sites)  $M$  of the spanning clusters. Using Eq. (4) we can find the fractal dimension of the spanning cluster and the magnetic exponent. The double logarithmic plot of  $M$  and  $L$  in Fig. 8 shows that the data is well described by a power law and an examination of different ranges of system size yields no clear trends in the power. A linear fit for  $L \geq 48$  yields  $\beta/\nu = 0.518 \pm .001$  consistent with a recent value  $0.5185 \pm .0008$  [8].

Next we consider the dynamical properties of the algorithm. The normalized autocorrelation function of an observable  $A$  is defined by,

$$\Gamma_A(t) = \frac{\langle A_0 A_t \rangle - \langle A \rangle^2}{\langle A^2 \rangle - \langle A \rangle^2}, \quad (6)$$

where  $t$  is time in Monte Carlo steps. Figure 9 shows the autocorrelation function for  $f$  for a  $128^3$  system. The striking feature of this curve is that it is negative on time step 1 indicating anti-correlations between successive MC steps. As discussed in Refs. [5,6,9] these anti-correlations are associated with the negative feedback mechanism that forces IC dynamics to the critical point. By the fourth step it is not possible to distinguish the autocorrelation function from zero.

The integrated autocorrelation time  $\tau_A$  is defined by,

$$\tau_A(w) = \frac{1}{2} + \sum_{t=1}^w \Gamma_A(t), \quad (7a)$$

$$\tau_A = \lim_{w \rightarrow \infty} \tau_A(w). \quad (7b)$$

Using the procedure described in Ref. [6], we measured integrated autocorrelation times for the magnetization  $m$ , energy  $\epsilon$  and temperature estimator  $f$ . The autocorrelation times are given in Table II and plotted against system size in Fig. 10. Due to these anti-correlations  $\tau_f$  and  $\tau_\epsilon$  *decrease* with system size;  $\tau_m$  remains nearly constant. Thus IC dynamics for the three-dimensional Ising model apparently does not suffer critical slowing. (Although, as is the case for all cluster algorithms, the parallel time needed for a single MC step must increase logarithmically with the system size [10]). The dynamic exponent  $z$  is defined by  $\tau \sim L^z$ . We obtained the dynamic exponents  $z_m = -.01 \pm .01$ ,  $z_\epsilon = -.46 \pm .01$  and  $z_f = -1.23 \pm .10$  for  $m$ ,  $\epsilon$  and  $f$  respectively.

Figure 11 shows  $\Gamma_f(1)$  as a function of  $1/L$ . It appears that the infinite volume limit for  $\Gamma_f(1)$  lies between between  $-0.6$  and  $-0.65$ . Since  $\tau_f \geq 0$  there must be corresponding positive values summing to at least  $0.1$  to  $0.15$  for  $t \geq 2$ . It would be interesting to have more information about the infinite volume limit of the  $f$  autocorrelation function.

The autocorrelation function is related to the standard error,  $\delta A$  in measuring  $\langle A \rangle$  according to,

$$\delta A = \sigma_A(2/N)^{1/2}(\tau_A - \frac{1}{N} \sum_{t=1}^{\infty} t\Gamma_A(t))^{1/2} \quad (8)$$

with  $\sigma_A^2 = \langle A^2 \rangle - \langle A \rangle^2$  and  $N$  the number of Monte Carlo steps. In most Monte Carlo applications the second term is much smaller than the first however for the IC algorithm this may not be the case since  $\tau_f, \tau_\epsilon \rightarrow 0$ . The autocorrelation function for  $f$  is approximately  $-1/2$  for  $t = 1$  and small for  $t > 1$  so that the approximate error in measuring the critical coupling is

$$\delta f \approx \sigma_f(2/N)^{1/2}(\tau_f + \frac{1}{2N})^{1/2}. \quad (9)$$

Suppose that the number of MC steps is large enough that  $\tau_f \gg 1/N$  as is the case here for the smaller system sizes. Combining the scaling behavior of  $\tau_f$  and of  $\sigma_f$  we have, for  $N \gg L^u$ ,

$$\delta f \sim L^{(z_f/2-u)}/N^{1/2} \sim L^{-1.31}/N^{1/2}. \quad (10)$$

On the other hand, if  $\tau_f$  and  $1/N$  are comparable as is the case here for the largest lattices then  $\delta f \sim L^{(z_f-u)} = L^{-1.92}$  and  $N \sim L^{-z_f} = L^{1.23}$ .

## V. CONCLUSIONS

We used a parallel implementation of the invaded cluster algorithm to study two- and three-dimensional Ising models. We have found that the parallel algorithm is quite efficient for large system sizes where most computational work is carried out constructing clusters within processing nodes and relatively little time is spent in communication.

We have shown that the invaded cluster algorithm has no critical slowing down for the three-dimensional Ising model as measured by integrated autocorrelation times for the magnetization, energy or estimated critical temperature. Indeed, the integrated autocorrelation time for the latter two quantities approaches zero as the system size grows so that relatively



few Monte Carlo steps are needed for high accuracy estimates of the finite-size critical energy or critical temperature.

On the other hand, extrapolation to the infinite volume limit for quantities such as the critical temperature is complicated by the absence of a well-understood finite-size scaling theory for the invaded cluster ensemble. We have examined the hypothesis that the distribution of  $f$  is controlled by a single scale factor and found that this apparently holds for large systems (greater than  $128^3$ ) but that there are significant corrections to the predicted asymptotic linear dependence of  $\langle f \rangle$  on  $\sigma_f$ . This is not unexpected since the width of the  $f$  distribution is rather large compared to  $|\langle f \rangle - p(K_c)|$ . Thus relatively small corrections to scaling for the  $f$  distribution can lead to relatively large deviations from the proposed linear behavior of  $\langle f \rangle$  vs.  $\sigma_f$ . This means that to confidently reduce systematic errors in estimating the infinite volume critical temperature we would either have to go to much larger systems to make  $\sigma_f$  small or we would need a detailed understanding of the corrections to scaling in the IC ensemble. Our current estimates of the critical temperature using the IC method are consistent with the best conventional estimates but have errors which are about an order of magnitude larger.

In contrast to the critical temperature, corrections to scaling in measuring the critical dimension of the spanning cluster are very small and we are able to obtain an excellent estimate of the magnetic exponent. Our result is  $y_h = 2.482 \pm .001$  ( $\beta/\nu = 0.518 \pm .001$ ).

#### ACKNOWLEDGMENTS

This work was supported in part by NSF Grant DMR-9632898.

## REFERENCES

- [1] R. H. Swendsen and J.-S. Wang. Nonuniversal critical dynamics in Monte Carlo simulations. *Phys. Rev. Lett.*, 58:86, 1987.
- [2] A. N. Burkitt and D. W. Heermann. *Comp. Phys. Comm.* 54:210, 1989. C. F. Baillie and P. D. Coddington. *Phys. Rev.* B43:10617, 1991. J. Kertesz and D. Stauffer. *Int. J. Mod. Phys.* C3:1275, 1992. J. Apostolakis, P. Coddington and E. Marinari. *Europhys. Lett.* 17:198, 1992. R. Hackl, H. -G. Mattutis, J. M. Singer, Th. Husslein and I. Morgenstein. *Physica* A212:277, 1994. G. T. Barkema and T. MacFarland. *Phys. Rev.* E50:1623, 1994.
- [3] P. Tamayo and M. Flanagan. Parallel cluster labelling for large-scale Monte Carlo simulations. *Physica*, A215:461, 1995.
- [4] R. Gupta and P. Tamayo. Critical exponents of the 3-D Ising model. *Int. Jour. of Mod. Phys.* C7:305, 1996.
- [5] J. Machta, Y. S. Choi, A. Lucke, T. Schweizer, and L. V. Chayes. Invaded cluster algorithm for equilibrium critical points. *Phys. Rev. Lett.*, 75:2792, 1995.
- [6] J. Machta, Y. S. Choi, A. Lucke, T. Schweizer, and L. M. Chayes. Invaded cluster algorithm for Potts models. *Phys. Rev. E*, 54:1332, 1996.
- [7] A. M. Ferrenberg, and D. P. Landau. Critical behavior of the three-dimensional Ising model: a high-resolution Monte Carlo study. *Phys. Rev.*, B44:5081, 1991.
- [8] H. W. J. Blote, E. Luijten, and J. R. Heringa. Ising universality in three dimensions: a Monte Carlo study. *J. Phys. A: Math. Gen.*, 28:6289, 1995.
- [9] T. B. Liverpool and S. C. Glotzer. Fixed cluster acceleration algorithm for spin systems. *Phys. Rev. E*, 53:R4255, 1996.
- [10] J. Machta and R. Greenlaw. The computational complexity of generating random fractals. *J. Stat. Phys.*, 82:1299, 1996.

## FIGURES

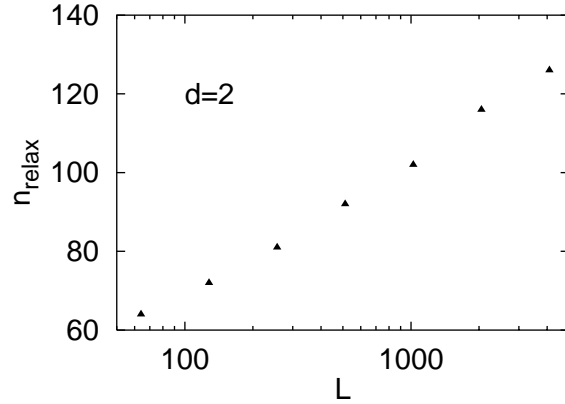


FIG. 1. The number of relaxation cycles per MC step  $n_{\text{relax}}$  vs. system size  $L$  for the two-dimensional Ising model.

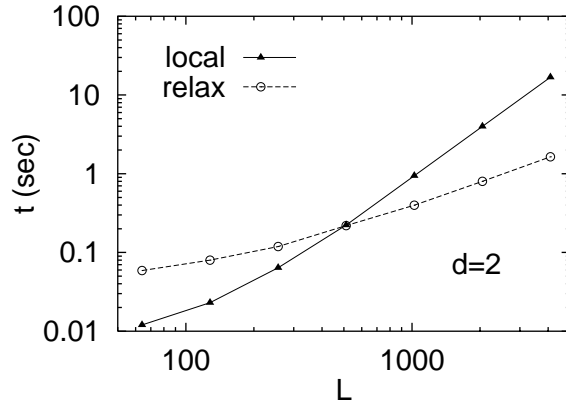


FIG. 2. Local time and relaxation time per MC step vs. system size  $L$  for the two-dimensional Ising model.

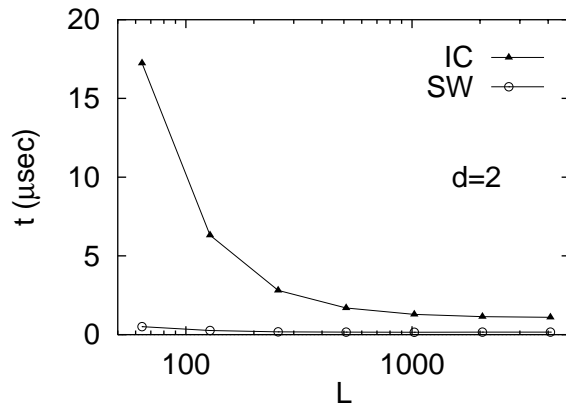


FIG. 3. Time per spin per MC step for the two-dimensional Ising model vs.  $L$  for the parallel IC and SW algorithms.

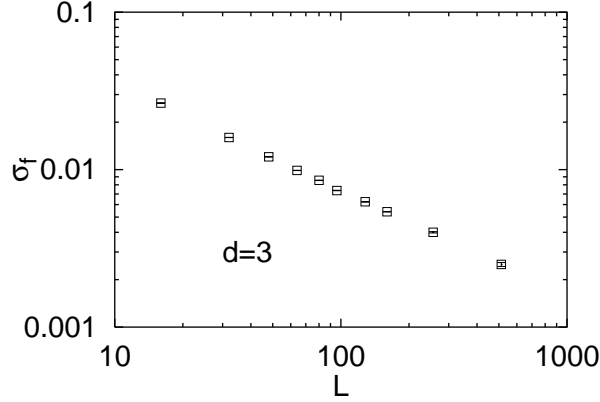


FIG. 4. Double logarithmic plot of  $\sigma_f$  vs. system size  $L$  for the three-dimensional Ising model. The slope of the curve is  $.69 \pm .01$  from a linear fit.

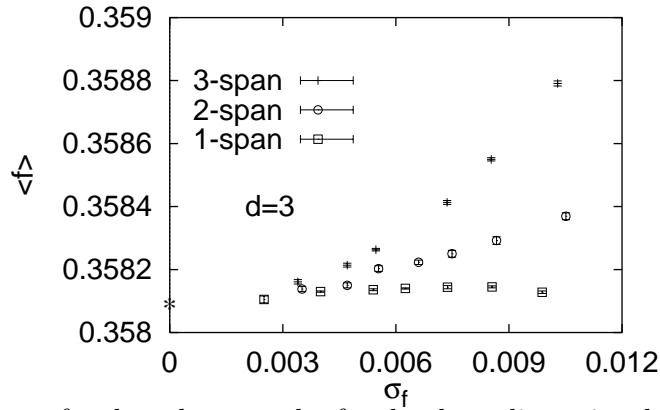


FIG. 5. Plot of  $f$  vs.  $\sigma_f$  for three  $k$ -span rules for the three-dimensional Ising model. The point on the vertical axis is the accepted infinite volume estimate.

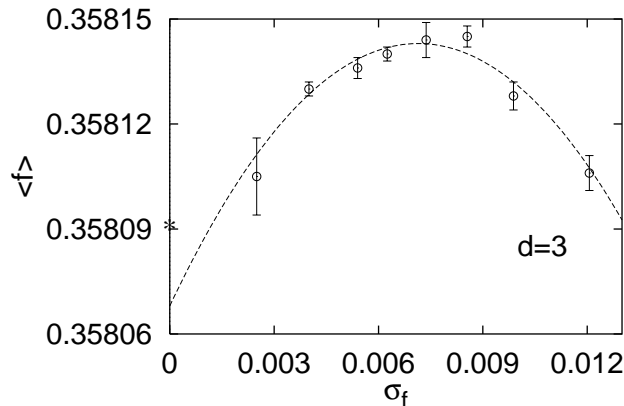


FIG. 6.  $\langle f \rangle$  vs.  $\sigma_f$  for the three-dimensional Ising model using the 1-span rule. The dotted line is a quadratic fit and yields  $p(K_c) = 0.358\,068 \pm .000009$ . The point on the vertical axis is the accepted infinite volume estimate.

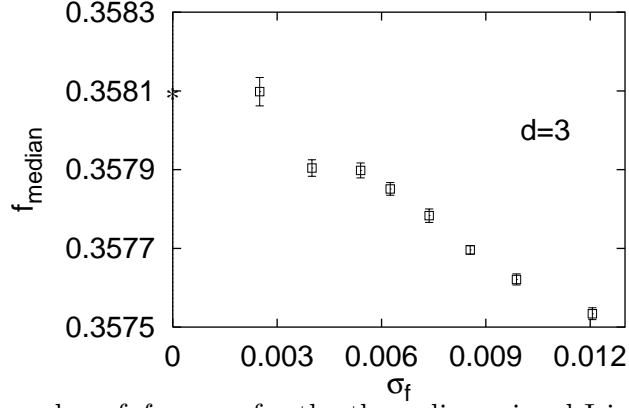


FIG. 7. The median value of  $f$  vs.  $\sigma_f$  for the three-dimensional Ising model using the 1-span rule.

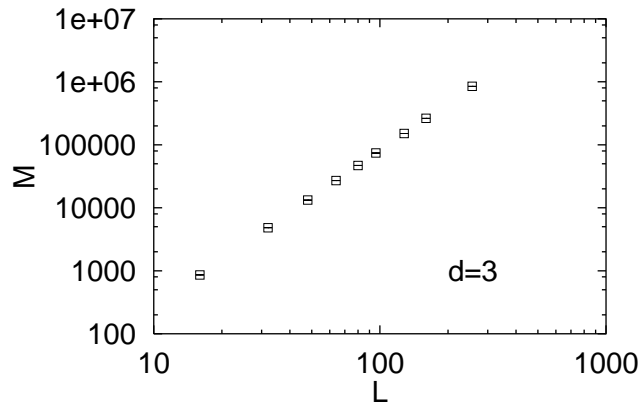


FIG. 8. Double logarithmic plot of the mass of the spanning cluster,  $M$  vs. system size  $L$  for the three-dimensional Ising model.

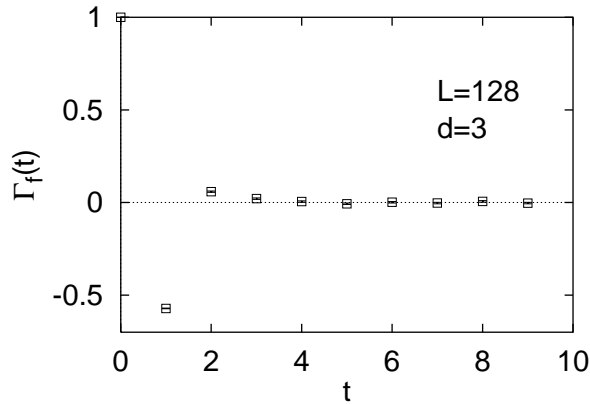


FIG. 9. Autocorrelation function for  $f$ ,  $\Gamma_f$  vs.  $t$  for the three-dimensional Ising model for system size  $128^3$ .

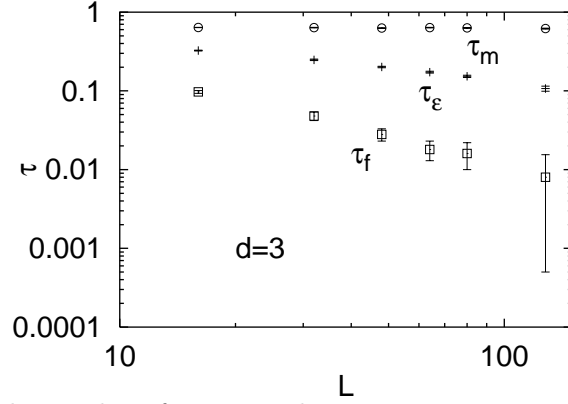


FIG. 10. Double logarithmic plot of autocorrelation times  $\tau_m, \tau_\epsilon, \tau_f$  vs. system size  $L$  for the three-dimensional Ising model.

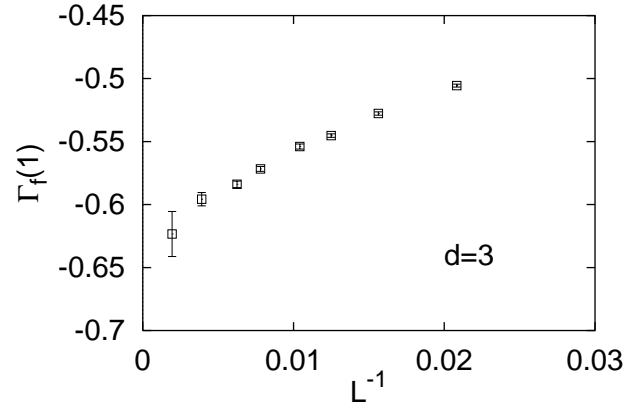


FIG. 11. Plot of  $\Gamma_f(1)$  vs.  $L^{-1}$  for the three-dimensional Ising model.

TABLES

TABLE I. Numerical data for the three-dimensional Ising model using the 1-span rule.

L	$\sigma_f$	$\langle f \rangle$	$f_{\text{median}}$	M	$\varepsilon$
16	.02645(4)	.357367(15)	.356223(33)	859(2)	-1.995544(57)
32	.01599(3)	.357961(11)	.357205(33)	4830(4)	-1.995055(26)
48	.01206(2)	.358106(5)	.357534(15)	13256(9)	-1.995242(23)
64	.00988(2)	.358128(4)	.357621(14)	27078(25)	-1.995289(25)
80	.00855(2)	.358145(3)	.357696(11)	47019(43)	-1.995339(19)
96	.00737(2)	.358144(5)	.357783(17)	74036(86)	-1.995362(33)
128	.00625(3)	.358140(2)	.357851(16)	151241(208)	-1.995377(18)
160	.00540(2)	.358136(3)	.357898(19)	263220(505)	-1.995389(15)
256	.00400(4)	.358130(2)	.357904(21)	847210(3238)	-1.995425(25)
512	.00250(7)	.358105(11)	.358098(36)	4668684(66195)	-1.995340(40)

TABLE II. Integrated autocorrelation times for three-dimensional Ising models for the IC algorithm. Results are measured at time step  $w = 6$ .

L	$\tau_\varepsilon$	$\tau_m$	$\tau_f$
16	.325(4)	.639(3)	.097(4)
32	.248(5)	.637(5)	.048(6)
48	.201(4)	.628(4)	.028(5)
64	.173(5)	.636(5)	.018(5)
80	.153(5)	.630(5)	.016(6)
128	.107(8)	.618(8)	.008(8)
160	.094(11)	.606(11)	.008(12)